Available online at www.sciencedirect.com

SCIENCE DIRECT®

International Journal of Solids and Structures 42 (2005) 6457–6474

INTERNATIONAL JOURNAL OF SOLIDS and STRUCTURES

www.elsevier.com/locate/ijsolstr

Study on wave localization in disordered periodic layered piezoelectric composite structures

Feng-Ming Li, Yue-Sheng Wang *

Institute of Engineering Mechanics, Beijing Jiaotong University, Haidian District, Beijing 100044, PR China

Received 23 July 2004; received in revised form 3 March 2005
Available online 12 April 2005

Abstract

The two-dimensional wave propagation and localization in disordered periodic layered 2-2 piezoelectric composite structures are studied by considering the mechanic-electric coupling. The transfer matrix between two consecutive sub-layers is obtained based on the continuity conditions. Regarding the variables of mechanical and electrical fields as the elements of the state vector, the expression of the localization factors in disordered periodic layered piezoelectric composite structures is derived. Numerical results are presented for two cases—disorder of the thickness of the polymers and disorder of the piezoelectric and elastic constants of the piezoelectric ceramics. The results show that due to the piezoelectric effects, the characteristics of the wave localization in disordered periodic layered piezoelectric composite structures are different from those in disordered periodic layered purely elastic ones. The wave localization is strengthened due to the piezoelectricity. And the larger the piezoelectric constant is, the larger the wave localization factors are. It is found that slight disorder in the piezoelectric or elastic constants of the piezoelectric ceramics can lead to more prominent localization phenomenon.

Keywords: Piezoelectricity; Disordered periodic structure; Wave localization; Localization factor; Transfer matrix

1. Introduction

Intelligent materials and structures possess the abilities of self-adaptive and active control. They can perceive the changes of outer environment and properly respond to these changes. Therefore, they are extensively used in many engineering applications (Hyland and Davis, 2002). Among various intelligent materials, piezoelectric composite materials are more and more widely applied, especially, in aeronautic

* Corresponding author. Tel.: +86 10 51688417; fax: +86 10 51682094.
E-mail address: yswang@center.njtu.edu.cn (Y.-S. Wang).

0020-7683/$ - see front matter © 2005 Elsevier Ltd. All rights reserved.
doi:10.1016/j.ijsolstr.2005.03.004

and astronautic engineering. Piezoelectric composites are made up of polymers and piezoelectric ceramics. They not only possess the merits of both polymers and piezoelectric ceramics but also greatly enhance the piezoelectric performances of the materials. So, piezoelectric composite materials are expected to be a main role in the development of future intelligent materials and structures.

Many piezoelectric composites and structures, which are extensively employed in intelligent materials and structures, have periodicity (cf. Castillero et al., 1998; Zinchuk and Podlipenets, 2001; Qian et al., 2004). Being different from non-periodic engineering structures, periodic ones have many special dynamic characteristics such as frequency passbands and stopbands (Baz, 2001). Furthermore, disordered periodic structures may also exhibit wave and vibration localization (Thorp et al., 2001; Li et al., 2002, 2004). Localization leads to a spatial decay of the wave amplitudes, and the associated exponential decay constant is known as the localization factor which characterizes the average exponential rates of decay of the wave amplitudes in disordered periodic structures. During the past decades, the special dynamic characteristics of periodic and disordered periodic structures have received considerable attention (Castanier and Pierre, 1995; Xie and Ibrahim, 2000; Zingales and Elishakoff, 2000).

However, most previous studies on the problem of wave or vibration localization were devoted to the case of purely elastic periodic structures. Few people have studied the periodic or disordered periodic piezoelectric structures which, we believe, are of practical importance in engineering. Baz (2001) and Thorp et al. (2001) investigated the problems of active vibration control and wave localization in the periodic spring–mass systems controlled by the piezoelectric actuators and rods with the periodic shunted piezoelectric patches and drew some significant conclusions.

In the present paper, the two-dimensional wave propagation and localization are studied in disordered periodic layered piezoelectric composite structures. The mechanic-electric coupling of piezoelectric materials are considered. Regarding the variables of the mechanical and electrical fields as the elements of the state vector, the formulation for calculating the localization factor in the disordered layered periodic structures is presented. Numerical results of the localization factors are presented for disorder in both the thickness of the polymers and the piezoelectric or elastic constants of the piezoelectric ceramics.

The paper is organized as follows. In Section 2, the equations of wave motion in piezoelectric composites are given. In Section 3, the transfer matrix between two consecutive unit cells is derived. The wave localization in the disordered system is studied in Section 4. Numerical results are presented in Section 5. The conclusions from this study are listed in Section 6.

2. Equations of wave motion

As shown in Fig. 1, a periodic layered 2-2 piezoelectric composite structure consists of the polymeric and piezoelectric ceramic thin films alternately. The thickness of the polymers and the piezoelectric ceramics are a_1 and a_2, respectively. The local coordinates of the polymeric film and those of the piezoelectric film are also displayed in the figure. Consider a steady anti-plane shear wave polarized in the z-direction propagating in the positive x-direction. Then the governing equations of SH-waves in the polymers and piezoelectric ceramics are written as (Qian et al., 2004)

$$c_{44}^{(1)}\nabla^2 w_1(x_1, y_1, t) - \rho_1 \frac{\partial^2 w_1(x_1, y_1, t)}{\partial t^2} = 0, \tag{1a}$$

$$\varepsilon_{11}^{(1)}\nabla^2 \varphi_1(x_1, y_1, t) = 0, \tag{1b}$$

$$c_{44}^{(2)}\nabla^2 w_2(x_2, y_2, t) + e_{15}^{(2)}\nabla^2 \varphi_2(x_2, y_2, t) - \rho_2 \frac{\partial^2 w_2(x_2, y_2, t)}{\partial t^2} = 0, \tag{2a}$$

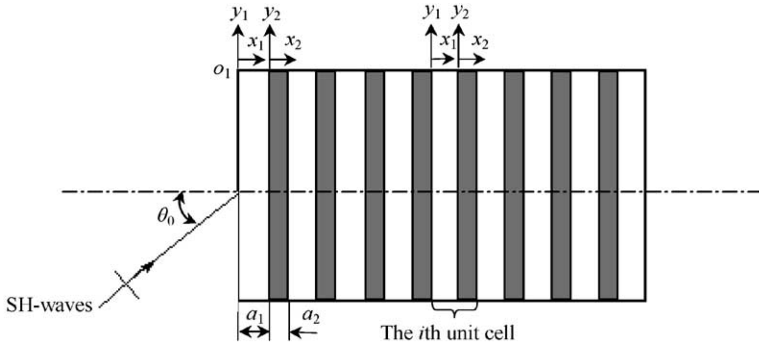

Fig. 1. Schematic diagram of a periodic layered 2-2 piezoelectric composite structure.

$$e_{15}^{(2)}\nabla^2 w_2(x_2, y_2, t) - \varepsilon_{11}^{(2)}\nabla^2\varphi_2(x_2, y_2, t) = 0, \tag{2b}$$

where $w_j(x_j, y_j, t)$ are the displacement components in z-direction, $\varphi_j(x_j, y_j, t)$ the electrical potential functions, ρ_j the mass densities, $c_{44}^{(j)}$ the elastic constants, and $\varepsilon_{11}^{(j)}$ the dielectric constants, with $j = 1$ referring to the polymers and $j = 2$ the piezoelectric ceramics; $e_{15}^{(2)}$ is the piezoelectric constant of the piezoelectric ceramics; ∇^2 is the Laplacian operator that is given by $\nabla^2 = \partial^2/\partial x_1^2 + \partial^2/\partial y_1^2$ in the polymers or $\nabla^2 = \partial^2/\partial x_2^2 + \partial^2/\partial y_2^2$ in the piezoelectric ceramics, respectively; and t is the time.

For an incident SH-wave polarized in the z-direction propagating in θ_0-direction as shown in Fig. 1, the harmonic solutions of displacement and electrical potential functions of Eqs. (1) and (2) can be written in the following forms:

$$w_j(x_j, y_j, t) = W_j(x_j)\exp[\mathrm{i}ky_j\sin\theta_0 - \mathrm{i}\omega t], \tag{3}$$

$$\varphi_j(x_j, y_j, t) = \Phi_j(x_j)\exp[\mathrm{i}ky_j\sin\theta_0 - \mathrm{i}\omega t], \tag{4}$$

where $j = 1, 2$; $\mathrm{i} = \sqrt{-1}$; $k = \omega/c$ is the wavenumber of the incident SH-wave; and ω and c are the circular frequency and phase velocity, respectively; W_j and Φ_j are the amplitudes of the displacements and electrical potentials, respectively; and θ_0 is the incident angle.

Substituting Eqs. (3) and (4) into Eqs. (1) and (2) yields

$$\frac{\mathrm{d}^2 W_1}{\mathrm{d}x_1^2} - k^2(\sin^2\theta_0 - k_1^2/k^2)W_1 = 0, \tag{5a}$$

$$\frac{\mathrm{d}^2 \Phi_1}{\mathrm{d}x_1^2} - k^2\sin^2\theta_0\Phi_1 = 0, \tag{5b}$$

$$\frac{\mathrm{d}^2 W_2}{\mathrm{d}x_2^2} - k^2(\sin^2\theta_0 - k_2^2/k^2)W_2 = 0, \tag{6a}$$

$$\frac{\mathrm{d}^2 \Phi_2}{\mathrm{d}x_2^2} - k^2\sin^2\theta_0\Phi_2 = p\left(\frac{\mathrm{d}^2 W_2}{\mathrm{d}x_2^2} - k^2\sin^2\theta_0 W_2\right), \tag{6b}$$

where $p = e_{15}^{(2)}/\varepsilon_{11}^{(2)}$ is the ratio of the piezoelectric constant to the dielectric constant of the piezoelectric ceramics; and k_1 and k_2 are, respectively, the wave numbers in the polymers and the piezoelectric ceramics with the forms

$$k_1 = \omega/c_1, \quad k_2 = \omega/c_2, \tag{7}$$

where c_1 and c_2 are the phase velocities of the bulk shear waves in the polymers and piezoelectric ceramics, respectively, and are given by

$$c_1 = \sqrt{\frac{c_{44}^{(1)}}{\rho_1}}, \quad c_2 = \sqrt{\frac{\left[c_{44}^{(2)}\varepsilon_{11}^{(2)} + (e_{15}^{(2)})^2\right]}{\rho_2\varepsilon_{11}^{(2)}}}. \tag{8}$$

In the following developments, it will be convenient to cast Eqs. (3)–(6) into dimensionless forms by introducing the following dimensionless local coordinates:

$$\xi_j = \frac{x_j}{\bar{a}_1}, \quad \eta_j = \frac{y_j}{\bar{a}_1} \quad (j = 1, 2), \tag{9}$$

where $\bar{a}_1$ is the mean value of the thickness of the piezoelectric ceramics. Substituting the first term of Eq. (9) into Eqs. (3)–(6) leads to the following non-dimensional equations:

$$w_j(\xi_j, \eta_j, t) = W_j(\xi_j)\exp[\mathrm{i}\alpha\eta_j \sin\theta_0 - \mathrm{i}\omega t] \quad (j = 1, 2), \tag{10}$$

$$\varphi_j(\xi_j, \eta_j, t) = \Phi_j(\xi_j)\exp[\mathrm{i}\alpha\eta_j \sin\theta_0 - \mathrm{i}\omega t] \quad (j = 1, 2), \tag{11}$$

$$\frac{\mathrm{d}^2 W_1}{\mathrm{d}\xi_1^2} - \alpha^2(\sin^2\theta_0 - \alpha_1^2/\alpha^2)W_1 = 0, \tag{12a}$$

$$\frac{\mathrm{d}^2 \Phi_1}{\mathrm{d}\xi_1^2} - \alpha^2\sin^2\theta_0\Phi_1 = 0 \quad (0 \leqslant \xi_1 \leqslant \zeta_1), \tag{12b}$$

$$\frac{\mathrm{d}^2 W_2}{\mathrm{d}\xi_2^2} - \alpha^2(\sin^2\theta_0 - \alpha_2^2/\alpha^2)W_2 = 0, \tag{13a}$$

$$\frac{\mathrm{d}^2 \Phi_2}{\mathrm{d}\xi_2^2} - \alpha^2\sin^2\theta_0\Phi_2 = p\left(\frac{\mathrm{d}^2 W_2}{\mathrm{d}\xi_2^2} - \alpha^2\sin^2\theta_0 W_2\right) \quad (0 \leqslant \xi_2 \leqslant \zeta_2), \tag{13b}$$

where $\alpha = k\bar{a}_1$ and $\alpha_j = k_j\bar{a}_1$ are the dimensionless wavenumbers and $\zeta_j = a_j/\bar{a}_1$ are the dimensionless thickness of the polymers and the piezoelectric ceramics.

The general solutions of Eqs. (12) and (13) are written as

$$W_1(\xi_1) = A_1\exp[-\mathrm{i}\alpha q_1\xi_1] + B_1\exp[\mathrm{i}\alpha q_1\xi_1], \tag{14a}$$

$$\Phi_1(\xi_1) = C_1\exp[-\alpha\sin\theta_0\xi_1] + D_1\exp[\alpha\sin\theta_0\xi_1], \tag{14b}$$

$$W_2(\xi_2) = A_2\exp[-\mathrm{i}\alpha q_2\xi_2] + B_2\exp[\mathrm{i}\alpha q_2\xi_2], \tag{15a}$$

$$\Phi_2(\xi_2) = C_2\exp[-\alpha\sin\theta_0\xi_2] + D_2\exp[\alpha\sin\theta_0\xi_2] + p\{A_2\exp[-\mathrm{i}\alpha q_2\xi_2] + B_2\exp[\mathrm{i}\alpha q_2\xi_2]\}, \tag{15b}$$

where $q_j = \sqrt{c^2/c_j^2 - \sin^2\theta_0}$ $(j = 1, 2)$; A_j, B_j, C_j and D_j $(j = 1, 2)$ are the unknown coefficients to be determined by the boundary conditions.

Substituting Eqs. (14) and (15) into Eqs. (10) and (11), we can see that the electrical potential function φ_1 in the polymers is exponentially attenuated along the thickness direction of the polymers. Other three terms, i.e. w_1,w_2 and φ_2, decay exponentially along the thickness direction of the piezoelectric ceramics layers in the case of $c/c_j < \sin\theta_0$. This case corresponds to the total reflection of elastic waves. So in this case the wave localization factors must be larger than zero and the corresponding frequency regions of elastic waves are stopbands. When $c/c_j \geqslant \sin\theta_0$, the terms of w_1, w_2 and φ_2 stand for the homogeneous plane waves that can propagate through the periodic layered composite structures without attenuation. The passbands and stopbands will appear in the corresponding frequency regions of the elastic waves.

For SH waves polarized in the z-direction, shear stresses and electrical displacements in the polymers and the piezoelectric ceramics can be respectively expressed as

$$\tau_{xz1} = c_{44}^{(1)}\frac{\partial w_1}{\partial x_1}, \quad D_{x1} = -\varepsilon_{11}^{(1)}\frac{\partial \varphi_1}{\partial x_1}, \tag{16}$$

$$\tau_{xz2} = c_{44}^{(2)}\frac{\partial w_2}{\partial x_2} + e_{15}^{(2)}\frac{\partial \varphi_2}{\partial x_2}, \quad D_{x2} = e_{15}^{(2)}\frac{\partial w_2}{\partial x_2} - \varepsilon_{11}^{(2)}\frac{\partial \varphi_2}{\partial x_2}. \tag{17}$$

3. Transfer matrix

Suppose that the periodic piezoelectric composite structure as shown in Fig. 1 consists of $n+1$ unit cells. Each unit cell includes two sub-cells (sub-cell 1 and sub-cell 2), namely, the polymeric and piezoelectric thin films. The boundary conditions at the left and right sides of the two sub-cells in the ith unit cell are written as

$$\begin{aligned}
&w_{1L}^{(i)} = w_1^{(i)}(0,\eta_1,t), \quad w_{1R}^{(i)} = w_1^{(i)}(\zeta_1,\eta_1,t),\\
&\tau_{xz1L}^{(i)} = c_{44}^{(1)}\frac{\partial w_1^{(i)}}{\partial \xi_1}(0,\eta_1,t), \quad \tau_{xz1R}^{(i)} = c_{44}^{(1)}\frac{\partial w_1^{(i)}}{\partial \xi_1}(\zeta_1,\eta_1,t),\\
&\varphi_{1L}^{(i)} = \varphi_1^{(i)}(0,\eta_1,t), \quad \varphi_{1R}^{(i)} = \varphi_1^{(i)}(\zeta_1,\eta_1,t),\\
&D_{x1L}^{(i)} = -\varepsilon_{11}^{(1)}\frac{\partial \varphi_1^{(i)}}{\partial \xi_1}(0,\eta_1,t), \quad D_{x1R}^{(i)} = -\varepsilon_{11}^{(1)}\frac{\partial \varphi_1^{(i)}}{\partial \xi_1}(\zeta_1,\eta_1,t) \quad (i=1,2,\ldots,n+1);
\end{aligned} \tag{18}$$

$$\begin{aligned}
&w_{2L}^{(i)} = w_2^{(i)}(0,\eta_2,t), \quad w_{2R}^{(i)} = w_2^{(i)}(\zeta_2,\eta_2,t),\\
&\tau_{xz2L}^{(i)} = c_{44}^{(2)}\frac{\partial w_2^{(i)}}{\partial \xi_2}(0,\eta_2,t) + e_{15}^{(2)}\frac{\partial \varphi_2^{(i)}}{\partial \xi_2}(0,\eta_2,t),\\
&\tau_{xz2R}^{(i)} = c_{44}^{(2)}\frac{\partial w_2^{(i)}}{\partial \xi_2}(\zeta_2,\eta_2,t) + e_{15}^{(2)}\frac{\partial \varphi_2^{(i)}}{\partial \xi_2}(\zeta_2,\eta_2,t),\\
&\varphi_{2L}^{(i)} = \varphi_2^{(i)}(0,\eta_2,t), \quad \varphi_{2R}^{(i)} = \varphi_2^{(i)}(\zeta_2,\eta_2,t),\\
&D_{x2L}^{(i)} = e_{15}^{(2)}\frac{\partial w_2^{(i)}}{\partial \xi_2}(0,\eta_2,t) - \varepsilon_{11}^{(2)}\frac{\partial \varphi_2^{(i)}}{\partial \xi_2}(0,\eta_2,t),\\
&D_{x2R}^{(i)} = e_{15}^{(2)}\frac{\partial w_2^{(i)}}{\partial \xi_2}(\zeta_2,\eta_2,t) - \varepsilon_{11}^{(2)}\frac{\partial \varphi_2^{(i)}}{\partial \xi_2}(\zeta_2,\eta_2,t) \quad (i=1,2,\ldots,n+1),
\end{aligned} \tag{19}$$

where the subscripts L and R denote the left and right sides of the two sub-cells in the ith unit cell.

Substitution of Eqs. (10), (11), (14) and (15) into Eqs. (18) and (19) leads to the following matrix equation:

$$\boldsymbol{v}_{jR}^{(i)} = T_j'\boldsymbol{v}_{jL}^{(i)} \quad (j=1,2;\, i=1,2,\ldots,n+1), \tag{20}$$

where $\boldsymbol{v}_{jR}^{(i)} = \left\{ w_{jR}^{(i)}, \tau_{xzjR}^{(i)}, \varphi_{jR}^{(i)}, D_{xjR}^{(i)} \right\}^{\mathrm{T}}$ and $\boldsymbol{v}_{jL}^{(i)} = \left\{ w_{jL}^{(i)}, \tau_{xzjL}^{(i)}, \varphi_{jL}^{(i)}, D_{xjL}^{(i)} \right\}^{\mathrm{T}}$ are the state vectors at the right and left sides of the two sub-cells and $\boldsymbol{T}_j'$ is the 4×4 transfer matrices of the two sub-cells. The elements of $\boldsymbol{T}_j'$ are given in Appendix A.

The following condition is satisfied at the interface between the two sub-cells:

$$\boldsymbol{v}_{1R}^{(i)} = \boldsymbol{v}_{2L}^{(i)}. \tag{21}$$

Thus the relationship between the right and left sides of the ith unit cell can be obtained from Eq. (20) as

$$\boldsymbol{v}_{2R}^{(i)} = \boldsymbol{T}_i \boldsymbol{v}_{1L}^{(i)} \quad (i = 2, \ldots, n+1), \tag{22}$$

where $\boldsymbol{T}_i$ is the transfer matrix of the ith unit cell and is given by

$$\boldsymbol{T}_i = \boldsymbol{T}_2' \boldsymbol{T}_1'. \tag{23}$$

At the interface between the right side of the $(i-1)$th unit cell and the left side of the ith unit cell, the following condition is satisfied:

$$\boldsymbol{v}_{1L}^{(i)} = \boldsymbol{v}_{2R}^{(i-1)} \quad (i = 2, \ldots, n+1). \tag{24}$$

Substituting Eq. (24) into Eq. (22), one can obtain the following relation between the state vectors of the $(i-1)$th and the ith unit cells:

$$\boldsymbol{v}_{2R}^{(i)} = T_i \boldsymbol{v}_{2R}^{(i-1)} \tag{25}$$

from which one can observe that T_i is the transfer matrix between two consecutive unit cells.

In order to analyze the influence of the piezoelectricity on the wave localization in the periodic 2-2 piezoelectric composite structures, the case of a periodic layered elastic structure without the piezoelectricity is also considered. By means of the same transfer matrix approach as mentioned above, the transfer matrices of the two sub-cells in each unit cell of the purely elastic structure can be derived and their elements are given in Appendix B. The vectors at the right and left sides of the two sub-cells are $\boldsymbol{v}_{jR}^{(i)} = \left\{ w_{jR}^{(i)}, \tau_{xzjR}^{(i)} \right\}^{\mathrm{T}}$ and $\boldsymbol{v}_{jL}^{(i)} = \left\{ w_{jL}^{(i)}, \tau_{xzjL}^{(i)} \right\}^{\mathrm{T}}$, respectively. The transfer matrix between two consecutive unit cells is also written by $\boldsymbol{T}_i = \boldsymbol{T}_2' \boldsymbol{T}_1'$. Therefore, if the piezoelectric effect is ignored in the periodic structures, the dimension of the transfer matrix is reduced to 2×2.

4. Wave localization

The Lyapunov exponent, which is a concept initially presented to characterize the temporal evolution of a dynamical system (Wolf et al., 1985), is defined as the average exponential rate of convergence or divergence between two neighboring phase orbits in the phase space and is considered as a measure of chaoticity. Therefore, the existence of a positive Lyapunov exponent implies that the dynamical system is instable. Localization factor, a similar concept applied to characterize the spatial evolution of a nearly periodic system (Castanier and Pierre, 1995) characterizes the average exponential rate of growth or decay of the wave amplitudes. So localization factors are related to the Lyapunov exponents of the corresponding discrete dynamical systems, Eq. (25). And, it has been proved that the largest Lyapunov exponent is equivalent to the localization factor for the mono-coupled system, while that the smallest positive Lyapunov exponent is the localization factor for the multi-coupled system (Kissel, 1991).

In the publications on disordered periodic systems, the transfer matrix formulation has been used extensively to determine the localization factors (Castanier and Pierre, 1995; Xie, 1998). For more detailed analysis on the numerical instabilities that appear by using the transfer matrix method in the study of wave propagation in multi-layered piezoelectric composites, one can refer to the papers written by Otero et al. (2004) and Rodríguez-Ramos et al. (2004).

As in Eq. (25), the state vector $\boldsymbol{v}_{2R}^{(i)}$ of the ith unit cell is related to that at the $(i-1)$th unit cell through the transfer matrix $\boldsymbol{T}_i$. Iteratively applying Eq. (25) from the first unit cell to the last one, i.e. the $(n+1)$th, unit cell, one can derive the relational expression between the state vectors $\boldsymbol{v}_{2R}^{(1)}$ and $\boldsymbol{v}_{2R}^{(n+1)}$ by a product of the transfer matrices

$$\boldsymbol{v}_{2R}^{(n+1)} = \boldsymbol{T}_{n+1}\boldsymbol{T}_n \cdots \boldsymbol{T}_2\boldsymbol{v}_{2R}^{(1)} = \boldsymbol{C}_n\boldsymbol{v}_{2R}^{(1)}, \tag{26}$$

where $\boldsymbol{C}_n = \boldsymbol{T}_{n+1}\boldsymbol{T}_n \cdots \boldsymbol{T}_2$ is called the total transfer matrix.

Following Wolf et al. (1985) for calculating Lyapunov exponents of continuous dynamical systems in temporal region, we define a Lyapunov exponent $\lambda(\boldsymbol{v}_{2R}^{(1)})$ depending on the initial vector $\boldsymbol{v}_{2R}^{(1)}$ for the discrete dynamical system, Eq. (25), in spatial region as follows:

$$\lambda(\boldsymbol{v}_{2R}^{(1)}) = \lim_{n\to\infty} \frac{1}{n} \ln \frac{\left\|\boldsymbol{v}_{2R}^{(n+1)}\right\|}{\left\|\boldsymbol{v}_{2R}^{(1)}\right\|}. \tag{27}$$

Depending on the choice of the initial state vector $\boldsymbol{v}_{2R}^{(1)}$, there will be d pairs of Lyapunov exponents having the following property:

$$\lambda_1 \geqslant \lambda_2 \geqslant \cdots \geqslant \lambda_d \geqslant \lambda_{d+1} \geqslant \cdots \geqslant \lambda_{2d}, \tag{28}$$

where $2d$ is the dimension of the transfer matrices $\boldsymbol{T}_{n+1} \cdots \boldsymbol{T}_2$.

Eq. (27) implies that for large number n, the following two relations:

$$\left\|\boldsymbol{v}_{2R}^{(n+1)}\right\| \approx \left\|\boldsymbol{v}_{2R}^{(1)}\right\| \exp(n\lambda) \quad \text{and} \quad \left\|\boldsymbol{v}_{2R}^{(1)}\right\| \approx \left\|\boldsymbol{v}_{2R}^{(n+1)}\right\| \exp(-n\lambda), \tag{29}$$

are equivalent. If the vectors $\boldsymbol{v}_{2R}^{(n+1)}$ and $\boldsymbol{v}_{2R}^{(1)}$ are respectively considered as the initial and the last state vectors, we can get from Eq. (27) that

$$\left\|\boldsymbol{v}_{2R}^{(1)}\right\| \approx \left\|\boldsymbol{v}_{2R}^{(n+1)}\right\| \exp(n\lambda). \tag{30}$$

From Eqs. (28)–(30) one can observe that the $2d$ Lyapunov exponents always occur in pairs, i.e. if λ_m is a Lyapunov exponent then $-\lambda_m$ is also a Lyapunov exponent. For $2d \times d$ transfer matrices, we arrange $\lambda_1, \lambda_2, \ldots, \lambda_{2d}$ in the descending order. Then the d pairs of Lyapunov exponents have the following property:

$$\lambda_1 \geqslant \lambda_2 \geqslant \cdots \geqslant \lambda_d \geqslant 0 \geqslant (\lambda_{d+1} = -\lambda_d) \geqslant (\lambda_{d+2} = -\lambda_{d-1}) \geqslant \cdots \geqslant (\lambda_{2d} = -\lambda_1), \tag{31}$$

where strict inequalities hold for disordered systems. In this case, the first halves of the Lyapunov exponents are positive, and the rest are negative.

For the mono-coupled disordered periodic system, there exist only one pair of waves and the dimension of the transfer matrices is 2×2. So there are only two Lyapunov exponents, namely, the positive one λ_1 and the negative one $-\lambda_1$. Therefore λ_1, the positive Lyapunov exponent, is the localization factor. For the multi-coupled case, there exist more than one pair of waves and each pair of waves have different transmission and reflection characteristics, and the dimension of the transfer matrices is $2d \times 2d$ ($d > 1$), higher than 2×2. So, there are d pairs of Lyapunov exponents in multi-coupled cases. And the smallest positive Lyapunov exponent λ_{d} represents the wave with potentially the least amount of decay, and so it carries energy along the periodic structure farther than any other waves and gives the dominant decay pattern. Hence, the smallest positive Lyapunov exponent λ_{d} is the localization factor.

In this paper, the algorithm developed by Wolf et al. (1985) for calculating Lyapunov exponents for continuous dynamical system is applied to the discrete dynamical system, Eq. (25). Assuming the dimension of the transfer matrices is $2d \times 2d$. In order to calculate the mth Lyapunov exponent ($1 \leqslant m \leqslant 2d$), m

orthogonal unit vectors of $2d$-dimension, $\boldsymbol{u}_1^{(1)}, \boldsymbol{u}_2^{(1)}, \ldots, \boldsymbol{u}_m^{(1)}$, are chosen as the initial state vectors. Then Eq. (25) is used to compute the state vectors iteratively. At the ith iteration,

$$\boldsymbol{v}_{2R,k}^{(i+1)} = \boldsymbol{T}_{i+1}\boldsymbol{u}_k^{(i)} \quad (i = 1, 2, \ldots n;\ k = 1, 2, \ldots, m), \tag{32}$$

where the vectors $\boldsymbol{u}_k^{(i)}$ are unit and orthogonal, while the vectors $\boldsymbol{v}_{2R,k}^{(i+1)} (k = 1, 2, \ldots, m)$ are usually not orthogonal. The Gram–Schmidt orthonormalization procedure is now applied to produce m orthogonal unit vectors

$$\begin{aligned}
&\hat{\boldsymbol{v}}_{2R,1}^{(i+1)} = \boldsymbol{v}_{2R,1}^{(i+1)}, \quad \boldsymbol{u}_1^{(i+1)} = \frac{\hat{\boldsymbol{v}}_{2R,1}^{(i+1)}}{\|\hat{\boldsymbol{v}}_{2R,1}^{(i+1)}\|},\\
&\hat{\boldsymbol{v}}_{2R,2}^{(i+1)} = \boldsymbol{v}_{2R,2}^{(i+1)} - (\boldsymbol{v}_{2R,2}^{(i+1)}, \boldsymbol{u}_1^{(i+1)})\boldsymbol{u}_1^{(i+1)}, \quad \boldsymbol{u}_2^{(i+1)} = \frac{\hat{\boldsymbol{v}}_{2R,2}^{(i+1)}}{\|\hat{\boldsymbol{v}}_{2R,2}^{(i+1)}\|},\\
&\ldots\\
&\hat{\boldsymbol{v}}_{2R,m}^{(i+1)} = \boldsymbol{v}_{2R,m}^{(i+1)} - (\boldsymbol{v}_{2R,m}^{(i+1)}, \boldsymbol{u}_{m-1}^{(i+1)})\boldsymbol{u}_{m-1}^{(i+1)} - \ldots - (\boldsymbol{v}_{2R,m}^{(i+1)}, \boldsymbol{u}_1^{(i+1)})\boldsymbol{u}_1^{(i+1)}, \quad \boldsymbol{u}_m^{(i+1)} = \frac{\hat{\boldsymbol{v}}_{2R,m}^{(i+1)}}{\|\hat{\boldsymbol{v}}_{2R,m}^{(i+1)}\|},
\end{aligned} \tag{33}$$

where $(\cdot,\cdot)$ denotes the dot-product.

After the m orthonormal unit vectors, $\boldsymbol{u}_1^{(i)}, \boldsymbol{u}_2^{(i)}, \ldots, \boldsymbol{u}_m^{(i)}$, are operated by transfer matrix $\boldsymbol{T}_{i+1}$ and orthonormalized by Gram–Schmidt procedure, the volume of an m-dimensional hypersphere is given by $\|\hat{\boldsymbol{v}}_{2R,1}^{(i+1)}\| \cdot \|\hat{\boldsymbol{v}}_{2R,2}^{(i+1)}\| \cdots \|\hat{\boldsymbol{v}}_{2R,m}^{(i+1)}\| = \prod_{k=1}^{m} \|\hat{\boldsymbol{v}}_{2R,k}^{(i+1)}\|$. Hence, after the initial vectors, $\boldsymbol{u}_1^{(1)}, \boldsymbol{u}_2^{(1)}, \ldots, \boldsymbol{u}_m^{(1)}$, are operated by a product of transfer matrices, $\boldsymbol{C}_n = \boldsymbol{T}_{n+1}\boldsymbol{T}_n \cdots \boldsymbol{T}_2$, the volume of an m-dimensional hypersphere becomes

$$V = \prod_{i=1}^{n}\left(\prod_{k=1}^{m} \|\hat{\boldsymbol{v}}_{2R,k}^{(i+1)}\|\right). \tag{34}$$

For an n-dimensional dynamical system in the phase space, an m-dimensional volume is defined by the m principal axes evolves on the average as

$$V = \exp[(\lambda_1 + \lambda_2 + \cdots + \lambda_m)n], \tag{35}$$

where $\lambda_1, \lambda_2, \ldots, \lambda_m$ are the m Lyapunov exponents. Hence, by combining Eq. (34) with (35), one can get the expression for determining the mth Lyapunov exponent as follows:

$$\lambda_m = \lim_{n\to\infty} \frac{1}{n} \sum_{i=1}^{n} \ln \|\hat{\boldsymbol{v}}_{2R,m}^{(i+1)}\|, \tag{36}$$

where n denotes the number of the iterations or the number of unit cells in the periodic structures.

By means of Eq. (36), each of the m pairs of Lyapunov exponents can be calculated. The mth Lyapunov exponent λ_m is the localization factor. For the periodic layered purely elastic structure, the dimension of the transfer matrices is 2×2 and then λ_1 is the localization factor. While for the periodic layered piezoelectric composite structure, the dimension of the transfer matrices is 4×4. So the second Lyapunov exponent, λ_2, is the localization factor.

5. Numerical examples and discussion

In this section, numerical computation for the randomly disordered periodic layered piezoelectric composite structure as shown in Fig. 1 is performed to examine the behavior of the propagation and localiza-

Table 1
Material constants of the polymers and piezoelectric ceramics

Maretials	Elastic constant c_{44} (10^{10} N/m^2)	Mass density ρ (10^3 kg/m^3)	Piezoelectric constant e_{15} (C/m^2)	Dielectric constant ε_{11} (10^{-10} F/m)
Polythene	0.128	1.18		0.2036
PZT-5H	2.30	7.50	17.0	277.0

tion of elastic waves with different frequencies. The non-dimensional thickness of the polymers, ζ_1, the piezoelectric and elastic constants of the piezoelectric ceramics, $e_{15}^{(2)}$ and $c_{44}^{(2)}$, are respectively considered disordered in calculations. As examples, we take the material constants of the polymers and piezoelectric ceramics from Qian et al. (2004) and list them in Table 1.

5.1. Disordered in the non-dimensional thickness of the polymers

The non-dimensional thickness of the polymers, ζ_1, is assumed to be a uniformly distributed random variable with the mean value, $\bar{\zeta}_1$, and the coefficient of variation, δ. So ζ_1 is a random number distributed in the interval $[\bar{\zeta}_1(1-\sqrt{3}\delta), \bar{\zeta}_1(1+\sqrt{3}\delta)]$. Introduce a standard uniformly distributed random variable, $r \in (0,1)$, then ζ_1 can be expressed as

$$\zeta_1 = \bar{\zeta}_1[1+\sqrt{3}\delta(2r-1)]. \tag{37}$$

The localization factors for the disordered periodic purely elastic and piezoelectric composite structures are respectively calculated by using Eq. (36). For the ith iteration, a random number r is generated to yield the dimensionless thickness of the polymers, and the elements of the transfer matrices are calculated. Three values of the coefficient of variation, i.e. $\delta = 0$, 0.05 and 0.1, are considered. The case of $\delta = 0$ corresponds to the perfectly periodic structures.

The case for $e_{15}^{(2)} = 0$ with other material constants listed in Table 1 is considered first. It is seen from Eq. (2) that the displacement and electrical potential functions in the piezoelectric ceramics are uncoupled in this case. The results are illustrated in Fig. 2 for wave incidence angle $\theta_0 = 0°$ (Fig. 2a) and 45° (Fig. 2b). For the purpose of comparison, the smallest positive Lyapunov exponent λ_2 for the periodic layered 2-2 piezoelectric structures with $e_{15}^{(2)} = 0$ and the positive Lyapunov exponent λ_1 for the periodic layered purely elastic structures are all plotted. The solid, dot-dashed and dashed lines denote the localization factor, λ_2, of the piezoelectric structures for $\delta = 0$, 0.05 and 0.1, respectively, and the scattered dots denote the localization factor, λ_1, of the purely elastic structures for the corresponding values of δ. It is clearly seen that the localization factor λ_1 for the purely elastic structures agrees extremely well with the smallest positive Lyapunov exponent λ_2 for the piezoelectric structures with $e_{15}^{(2)} = 0$. This fact implies that the results for the purely elastic structures (2×2 transfer matrices) can be recovered from those for the piezoelectric structures (4×4 transfer matrices) by setting $e_{15}^{(2)} = 0$.

It is also seen from Fig. 2 that ordered periodic structures ($\delta = 0$) have the properties of frequency passbands and stopbands while that a localization phenomenon occurs in disordered periodic structures. For example, as shown by the solid lines in Fig. 2b, the interval $\alpha \in (2.2, 2.6)$ where the localization factors vanish is known as the passband; and the interval $\alpha \in (2.6, 4.3)$ is called the stopband as the localization factors are bigger than zero at this frequency region. Moreover, the localization factors in the disordered periodic structures are not zero but positive in the passbands of the corresponding ordered periodic ones, which means that elastic waves cannot be freely transmitted but localized. With the increase of the coefficient of variation δ, the amplitudes of the localization factors in the passbands are increased and thus the localization is strengthened.

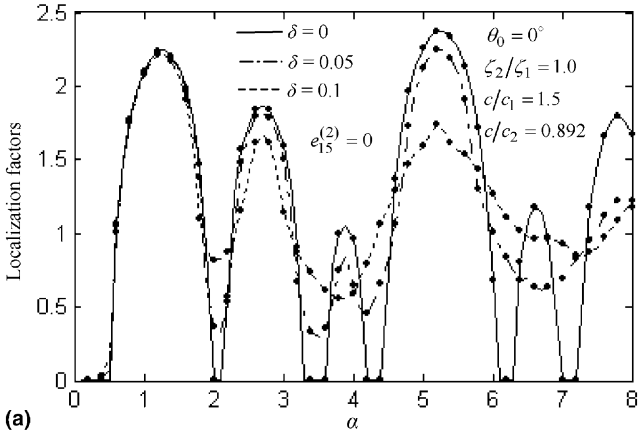

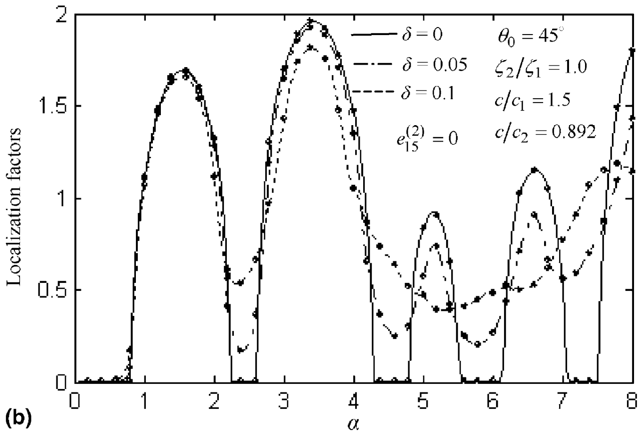

Fig. 2. Localization factors vs. non-dimensionalized wave number α for $e_{15}^{(2)} = 0$ with comparison to the results of periodic purely elastic structures.

Fig. 3 shows effects of the incident angles on the localization factors of the disordered piezoelectric structures. Comparing Fig. 3 with Fig. 2, we can find that the localization behavior of the disordered periodic piezoelectric structures changes pronouncedly for different incident angles. For instance, when $\theta_0 < 30°$ (Fig. 3a–c), with the increase of the incident angle the peak values of the localization factors are decreased and the passbands for ordered periodic structures are gradually broadened. However, when θ_0 increases to 70° (Fig. 3c), an interesting phenomenon appears: the localization factors are all positive even for the ordered periodic structures except for a single frequency point in the considered frequency regions. This is understood by considering that total reflection of elastic waves occurs in this case because $\sin\theta_0 = 0.940 > c/c_2 = 0.543$ for $\theta_0 = 70°$. Therefore no passband appears in this case even for ordered periodic structures.

In order to analyze the effects of the piezoelectric effects on the dynamical behavior of the wave propagation and localization, the localization factors for different values of $e_{15}^{(2)}$ (0, 5, 10 and 20 C/m^2) with other material constants as listed in Table 1 are computed and illustrated in Fig. 4 as functions of α for both ordered (Fig. 4a) and disordered (Fig. 4b) periodic structures. We can see from Fig. 4a that with the increase of $e_{15}^{(2)}$, the peak values of localization factors also increase and passbands for ordered periodic

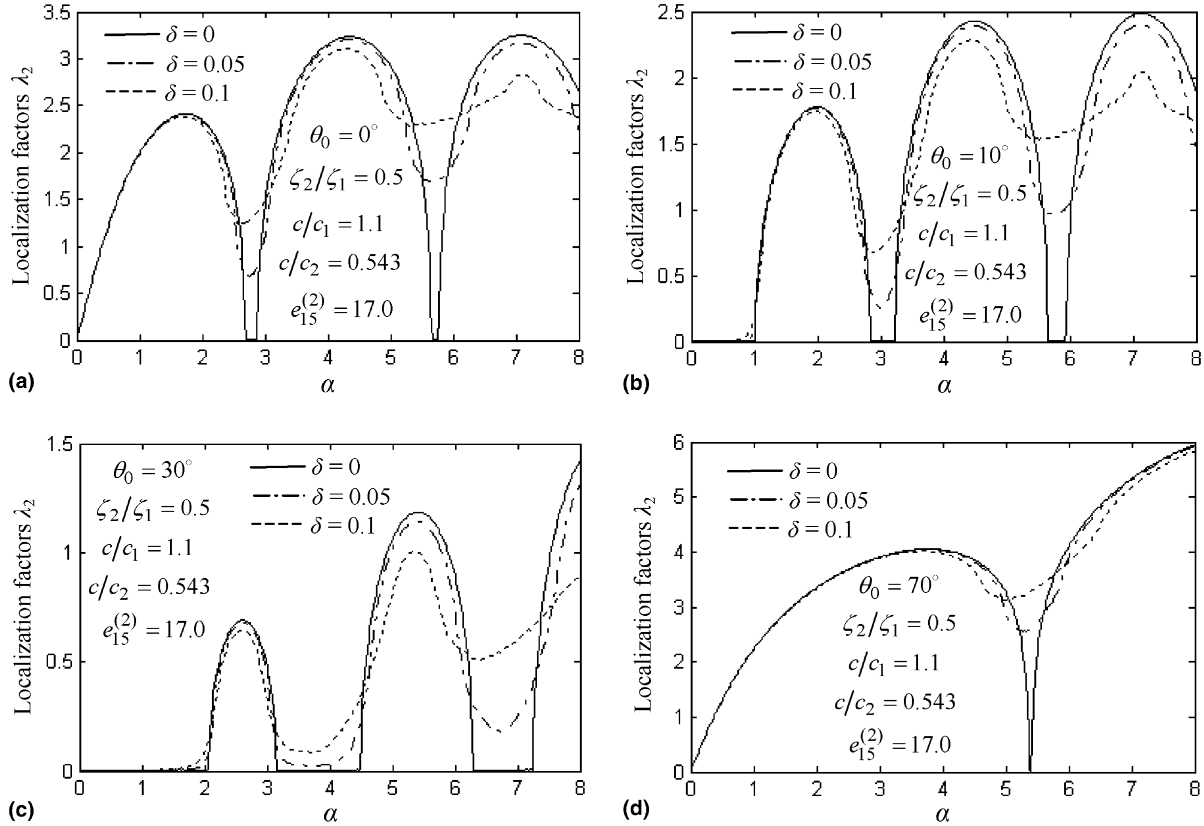

Fig. 3. Localization factors vs. non-dimensionalized wave number α with the consideration of the effects of incident angle θ_0.

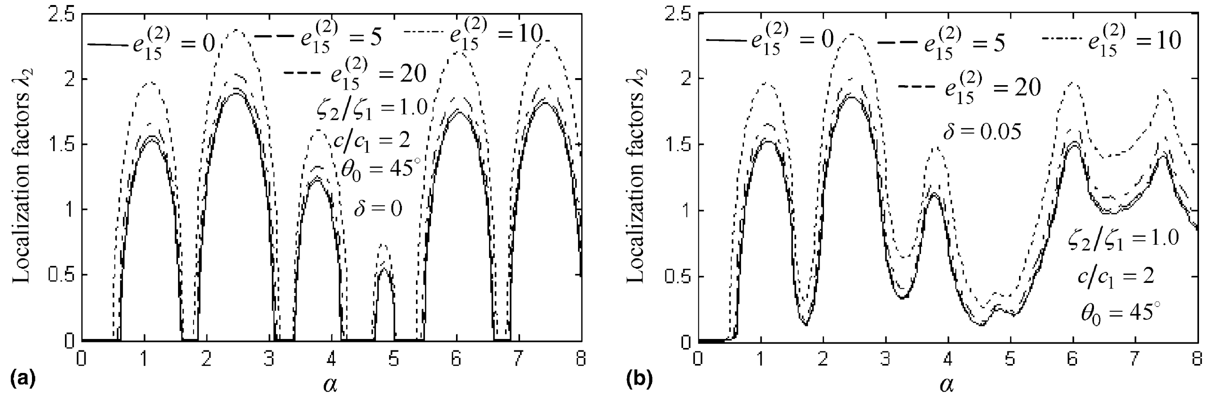

Fig. 4. Localization factors vs. non-dimensionalized wave number α with the consideration of the effects of $e_{15}^{(2)}$ for $\delta = 0$ (a) and $\delta = 0.05$ (b).

structures become narrower. This means that the piezoelectricity increases the widths of the stopbands, and thus fewer waves can propagate through the structures.

It is observed from Fig. 4b that for disordered periodic structures the localization factors are positive in almost all the considered frequency regions. With the increase of $e_{15}^{(2)}$, the peak values of localization factors also increase and the localization factors of the piezoelectric structures are larger than those of the purely elastic ones (solid lines). So we could conclude that the wave localization in the disordered periodic piezoelectric structures is stronger than that in the disordered periodic purely elastic ones. And the larger the piezoelectric constant of the piezoelectric ceramics is, the stronger the wave localization is.

Fig. 5 shows the variations of localization factors vs. non-dimensional wave-number α with the consideration of the effects of c/c_1 (or equivalently c/c_2 since c/c_2 can be determined from Eq. (8) and Table 1 for a given value of c/c_1) for $\zeta_2/\zeta_1 = 1.0$, $\theta_0 = 30°$ and $\delta = 0$, 0.05 and 0.1. We can see that for the case of $c/c_1 = 0.5$ (or $c/c_2 = 0.247$, the case of $c/c_1 \neq 1$ implies that the SH-waves are incident to the piezoelectric composite from other media conglutinated to it) the localization factors for ordered and disordered periodic structures are positive in all frequency regions and gradually increase with the increase of α. This phenomenon is due to the fact that $\sin\theta_0 = 0.5 > c/c_2 = 0.247$ and thus the total reflection of elastic waves appears. Therefore all frequency regions are stopbands and no elastic waves can propagate through the periodic or disordered periodic piezoelectric structures. With the increase of c/c_1 or c/c_2, it is observed that the passbands appear for ordered periodic structures and wave localization phenomenon occurs for disordered structures. It can also be seen from Figs. 5b–d that with the increase of c/c_1 or c/c_2, the pass-

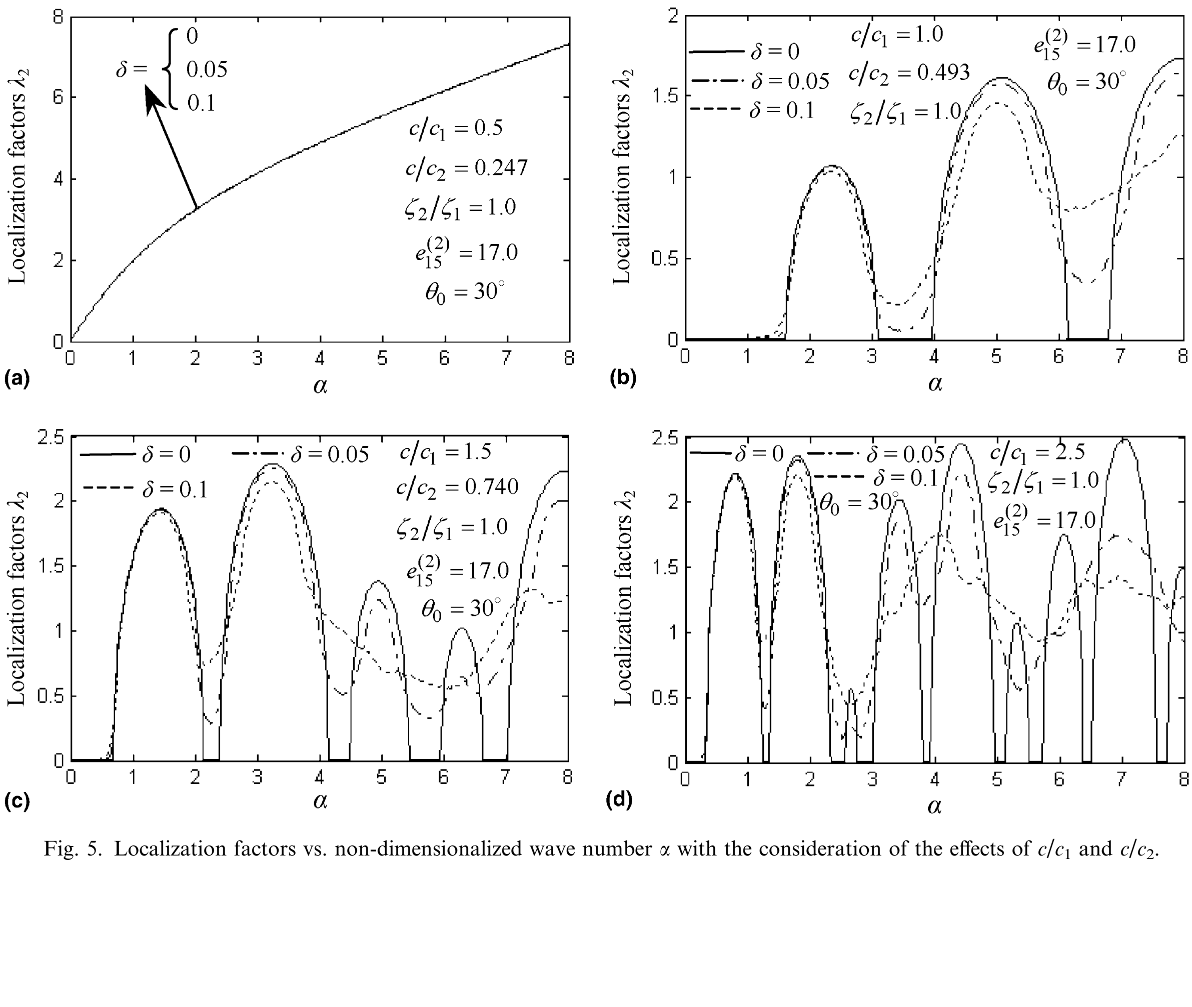

Fig. 5. Localization factors vs. non-dimensionalized wave number α with the consideration of the effects of c/c_1 and c/c_2.

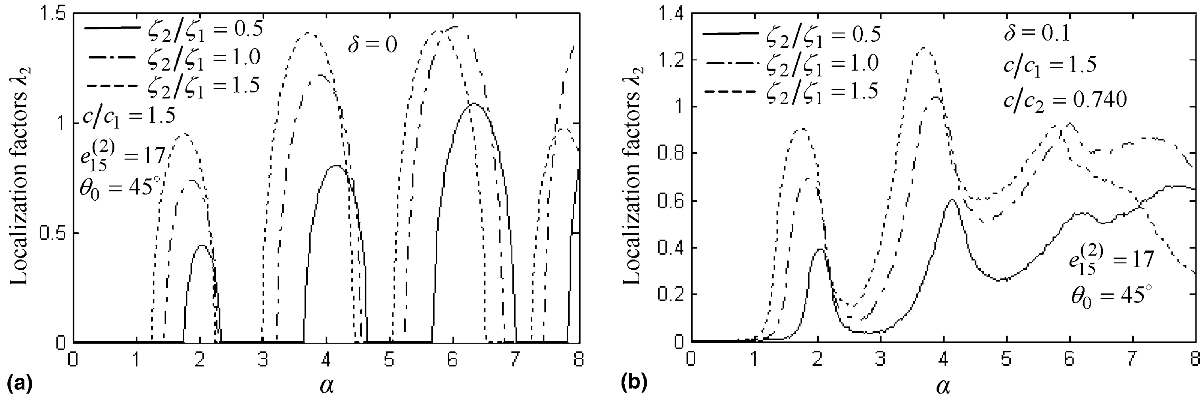

Fig. 6. Localization factors vs. non-dimensionalized wave number α with the consideration of the effects of ζ_2/ζ_1 for $\delta = 0$ (a) and $\delta = 0.1$ (b).

bands become narrower, the stopbands become broader, and the number of passband and stopband is increased.

The variations of the localization factors vs. non-dimensional wave-number α with the consideration of the effects of the thickness of the piezoelectric ceramics for $c/c_1 = 1.5$ (or $c/c_2 = 0.740$), $\theta_0 = 45°$ and $\delta = 0$ and 0.1 are displayed in Fig. 6. It can be observed from Fig. 6a that the passbands near $\alpha = 0$ and 3.0 become narrower and that the widths of the passbands near $\alpha = 5.0$ and 7.0 have little changes for different values of ζ_2/ζ_1. However the locations of the passbands have more changes with the increase of ζ_2/ζ_1. We can see from Fig. 6b that for disordered periodic structures the localization factors increase with the increase of ζ_2/ζ_1 in the interval of $\alpha \in (1.0, 5.8)$ and that the localization factor for the case of $\zeta_2/\zeta_1 = 1.5$ decrease rapidly with the increase of α when $\alpha > 5.8$.

5.2. Disorder in the piezoelectric and elastic constants of the piezoelectric ceramics

In this section, the piezoelectric constant $e_{15}^{(2)}$ and the elastic constant $c_{44}^{(2)}$ of the piezoelectric ceramics are respectively assumed disordered to discuss the localization of SH-waves in the disordered periodic 2-2 piezoelectric composite structures. The piezoelectric and elastic constants of the piezoelectric ceramics are considered to be uniformly distributed random variables which may be expressed as

$$Z = \overline{Z}[1 + \sqrt{3}\delta(2r - 1)], \tag{38}$$

where Z stands for $e_{15}^{(2)}$ or $c_{44}^{(2)}$; $\overline{Z}$ is the mean value of $e_{15}^{(2)}$ or $c_{44}^{(2)}$; δ is the coefficient of variance of $e_{15}^{(2)}$ or $c_{44}^{(2)}$; and r is a standard uniformly distributed random variable.

Figs. 7 and 8 shows the variations of localization factors vs. dimensionless wave-number α with the disordered piezoelectric and elastic constants of the piezoelectric ceramics, respectively. In Fig. 7 the mean value of the piezoelectric constant is taken as $\overline{e}_{15}^{(2)} = 17.0\ \mathrm{C/m^2}$, the incident angle θ_0 are 30° and 45°, the coefficient of variation $\delta = 0$, 0.002, 0.005 and 0.01 and the other parameters are shown in the figure. From Fig. 7a we can clearly observe that with the increase of δ the localization factors in the passband of $\alpha \in (5.5, 6.0)$ are positive and increased. In Fig. 7b we can see that with the increase of δ the passbands in the lower frequency regions become narrower and the localization phenomenon appear in the higher frequency regions. In Fig. 8 the mean value of the elastic constant is taken as $\overline{c}_{44}^{(2)} = 2.30 \times 10^{10}\ \mathrm{N/m^2}$. Similar phenomenon as in Fig. 7 is observed. The most important feature that shown in Figs. 7 and 8 is that for

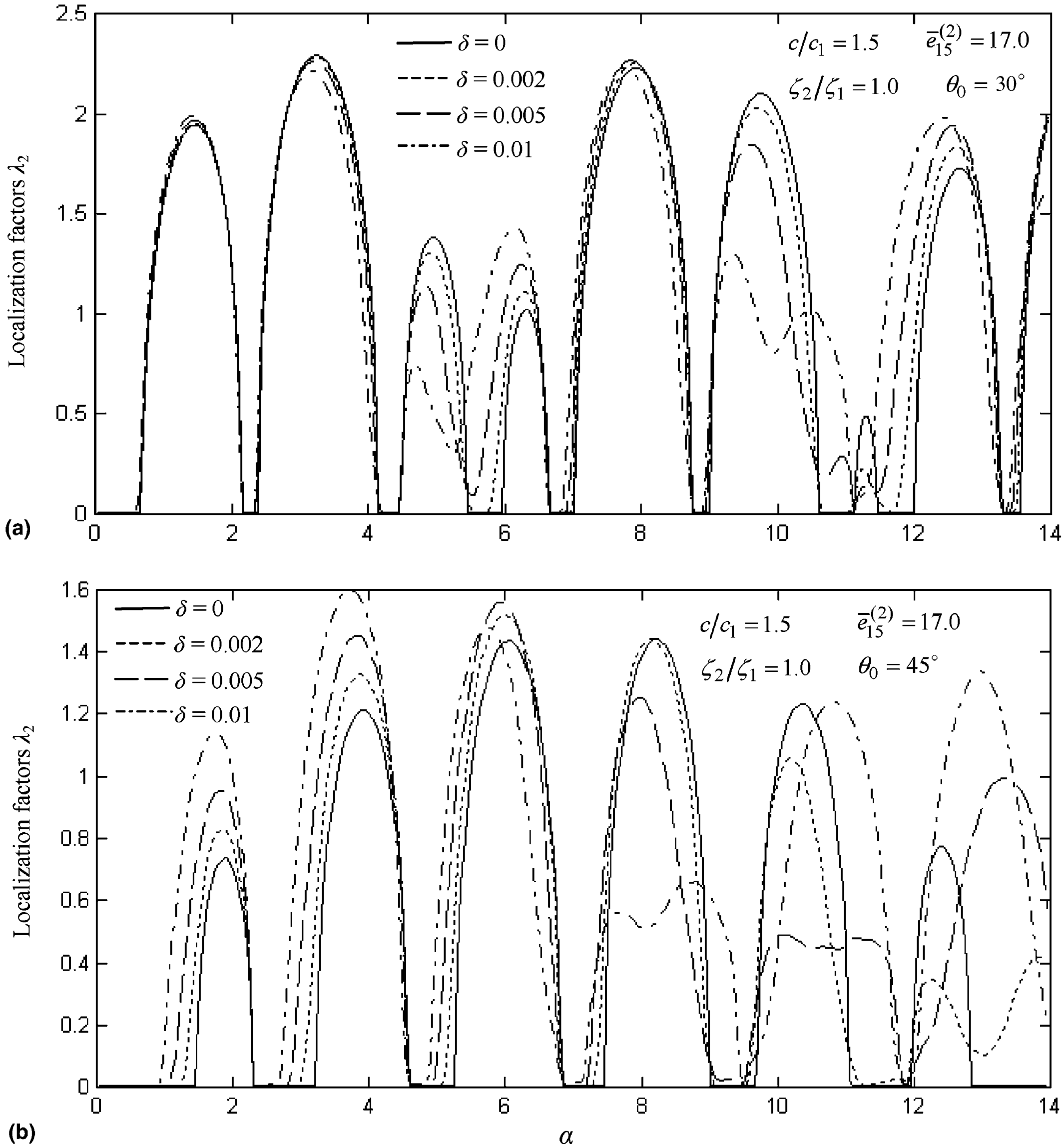

Fig. 7. Localization factors vs. non-dimensionalized wave number α for the case of the piezoelectric constant of the piezoelectric ceramics assumed to be disordered.

very small disorder ($\delta = 0.002$ and 0.005) the localization phenomenon is more pronounced. So even slight disorder of the piezoelectric or elastic constants of the piezoelectric ceramics has remarkable influences on the dynamical behaviors of disordered periodic piezoelectric composite structures and cannot be ignored. The reason why slight disorder of the piezoelectric or elastic constant of the piezoelectric ceramics can lead to more prominent localization phenomenon is that slight disorder can result in larger variation of the bulk shear wave velocity, and therefore remarkable changes of the wave behaviors, in the piezoelectric ceramics, see Eq. (8).

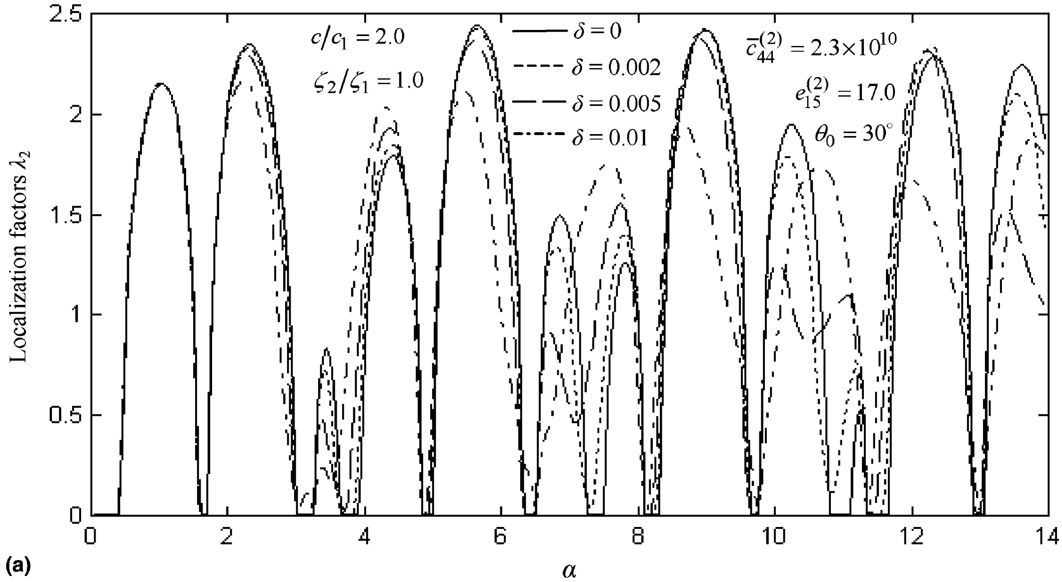

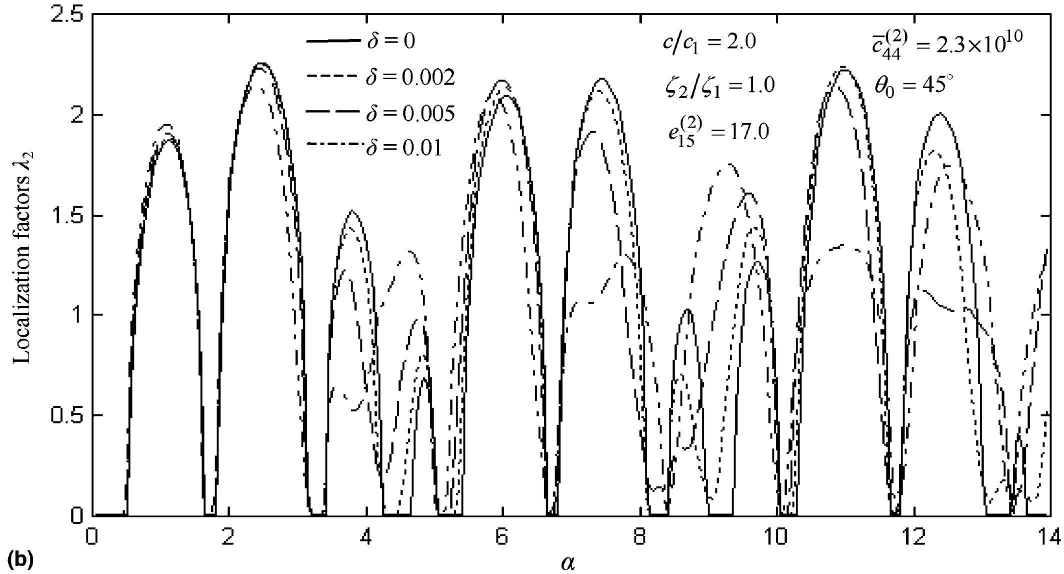

Fig. 8. Localization factors vs. non-dimensionalized wave number α for the case of the elastic constant of the piezoelectric ceramics assumed to be disordered.

6. Conclusions

In the present work, the two-dimensional wave propagation and localization in disordered periodic layered 2-2 piezoelectric composite structures are studied with the consideration of the mechanical and electrical coupling. The transfer matrix between two consecutive sub-layers is obtained based on the continuity conditions at the interfaces and the expression of the localization factor in disordered periodic structures is presented. For the purpose of comparison, the case of the piezoelectric constant of the piezoelectric ceramics, $e_{15}^{(2)}$, being equal to zero is also considered. Numerical simulations are performed to calculate the localization factors for disorders in both the non-dimensional thickness of the polymers and the piezoelectric or elastic constants of the piezoelectric ceramics. From the results, we can draw the following conclusions:

(1) For a periodic layered piezoelectric composite structure, the dimension of the transfer matrix is 4×4, and the smallest positive Lyapunov exponent λ_2 is the localization factor. But if the piezoelectric constant of the piezoelectric ceramics is equal to zero, the dimension of the transfer matrix is reduced to 2×2, and the positive Lyapunov exponent λ_1 is the localization factor. This special case is identical to the case of periodic purely elastic structures.
(2) Tuned periodic structures have the properties of frequency passbands and stopbands and a localization phenomenon can occur in mistuned periodic ones. The larger the coefficient of variation is, the stronger the localization is.
(3) Due to the effect of piezoelectricity, the wave localization in disordered periodic layered piezoelectric structures is stronger than that in disordered periodic purely elastic ones. With the increase of the piezoelectric constant, the wave localization becomes more pronounced.
(4) Slight disorder of the piezoelectric or elastic constant of the piezoelectric ceramics can lead to more prominent localization phenomenon.
(5) The behavior of the wave propagation and localization may be controlled by properly adjusting the value of the piezoelectric constants.

Acknowledgments

The authors wish to express gratitude for the support provided by the National Science Fund for Distinguished Young Scholars under Grant no. 10025211. The first author is also grateful to the support by the NJTU Paper Foundation of China under Grant no. PD249 and the China Postdoctoral Science Foundation.

Appendix A

The elements of the transfer matrices of two sub-cells in the ith unit cell of disordered periodic layered piezoelectric composite structures are written as

$$
\begin{aligned}
&T_1'(1,1) = \frac{\exp(-\mathrm{i}\alpha q_1 \zeta_1) + \exp(\mathrm{i}\alpha q_1 \zeta_1)}{2}, \quad T_1'(1,2) = \frac{\exp(\mathrm{i}\alpha q_1 \zeta_1) - \exp(-\mathrm{i}\alpha q_1 \zeta_1)}{2\mathrm{i}\alpha q_1 c_{44}^{(1)}},\\
&T_1'(1,3) = 0, \quad T_1'(1,4) = 0, \quad T_1'(2,1) = \frac{\mathrm{i}\alpha q_1 c_{44}^{(1)}[\exp(\mathrm{i}\alpha q_1 \zeta_1) - \exp(-\mathrm{i}\alpha q_1 \zeta_1)]}{2},\\
&T_1'(2,2) = \frac{\exp(-\mathrm{i}\alpha q_1 \zeta_1) + \exp(\mathrm{i}\alpha q_1 \zeta_1)}{2}, \quad T_1'(2,3) = 0, \quad T_1'(2,4) = 0,\\
&T_1'(3,1) = 0, \quad T_1'(3,2) = 0, \quad T_1'(3,3) = \frac{\exp(-\alpha \zeta_1 \sin\theta_0) + \exp(\alpha \zeta_1 \sin\theta_0)}{2},\\
&T_1'(3,4) = \frac{\exp(-\alpha \zeta_1 \sin\theta_0) - \exp(\alpha \zeta_1 \sin\theta_0)}{2\alpha \varepsilon_{11}^{(1)} \sin\theta_0}, \quad T_1'(4,1) = 0,
\end{aligned}
\tag{A.1}
$$

$$T_1'(4,2)=0,\quad T_1'(4,3)=\frac{\alpha\varepsilon_{11}^{(1)}\sin\theta_0[\exp(-\alpha\zeta_1\sin\theta_0)-\exp(\alpha\zeta_1\sin\theta_0)]}{2},$$
$$T_1'(4,4)=\frac{\exp(-\alpha\zeta_1\sin\theta_0)+\exp(\alpha\zeta_1\sin\theta_0)}{2};$$

$$T_2'(1,1)=\frac{\exp(-\mathrm{i}\alpha q_2\zeta_2)+\exp(\mathrm{i}\alpha q_2\zeta_2)}{2},\quad T_2'(1,2)=\frac{\exp(\mathrm{i}\alpha q_2\zeta_2)-\exp(-\mathrm{i}\alpha q_2\zeta_2)}{2\mathrm{i}\alpha q_2[pe_{15}^{(2)}+c_{44}^{(2)}]},$$
$$T_2'(1,3)=0,\quad T_2'(1,4)=\frac{p[\exp(\mathrm{i}\alpha q_2\zeta_2)-\exp(-\mathrm{i}\alpha q_2\zeta_2)]}{2\mathrm{i}\alpha q_2[pe_{15}^{(2)}+c_{44}^{(2)}]},$$
$$T_2'(2,1)=\frac{\mathrm{i}\alpha q_2[pe_{15}^{(2)}+c_{44}^{(2)}][\exp(\mathrm{i}\alpha q_2\zeta_2)-\exp(-\mathrm{i}\alpha q_2\zeta_2)]}{2}+\frac{p\alpha e_{15}^{(2)}\sin\theta_0[\exp(-\alpha\zeta_2\sin\theta_0)-\exp(\alpha\zeta_2\sin\theta_0)]}{2},$$
$$T_2'(2,2)=\frac{\exp(-\mathrm{i}\alpha q_2\zeta_2)+\exp(\mathrm{i}\alpha q_2\zeta_2)}{2},$$
$$T_2'(2,3)=\frac{\alpha e_{15}^{(2)}\sin\theta_0[\exp(\alpha\zeta_2\sin\theta_0)-\exp(-\alpha\zeta_2\sin\theta_0)]}{2},$$
$$T_2'(2,4)=\frac{p[\exp(\mathrm{i}\alpha q_2\zeta_2)+\exp(-\mathrm{i}\alpha q_2\zeta_2)-\exp(\alpha\zeta_2\sin\theta_0)-\exp(-\alpha\zeta_2\sin\theta_0)]}{2},$$
$$T_2'(3,1)=\frac{p[\exp(\mathrm{i}\alpha q_2\zeta_2)+\exp(-\mathrm{i}\alpha q_2\zeta_2)-\exp(\alpha\zeta_2\sin\theta_0)-\exp(-\alpha\zeta_2\sin\theta_0)]}{2},$$
$$T_2'(3,2)=\frac{p[\exp(\mathrm{i}\alpha q_2\zeta_2)-\exp(-\mathrm{i}\alpha q_2\zeta_2)]}{2\mathrm{i}\alpha q_2[pe_{15}^{(2)}+c_{44}^{(2)}]},\quad T_2'(3,3)=\frac{\exp(-\alpha\zeta_2\sin\theta_0)+\exp(\alpha\zeta_2\sin\theta_0)}{2},$$
$$T_2'(3,4)=\frac{p^2[\exp(\mathrm{i}\alpha q_2\zeta_2)-\exp(-\mathrm{i}\alpha q_2\zeta_2)]}{2\mathrm{i}\alpha q_2[pe_{15}^{(2)}+c_{44}^{(2)}]}+\frac{\exp(-\alpha\zeta_2\sin\theta_0)-\exp(\alpha\zeta_2\sin\theta_0)}{2\alpha\varepsilon_{11}^{(2)}\sin\theta_0},$$
$$T_2'(4,1)=\frac{\alpha e_{15}^{(2)}\sin\theta_0[\exp(\alpha\zeta_2\sin\theta_0)-\exp(-\alpha\zeta_2\sin\theta_0)]}{2},$$
$$T_2'(4,2)=0,\quad T_2'(4,3)=\frac{\alpha\varepsilon_{11}^{(2)}\sin\theta_0[\exp(-\alpha\zeta_2\sin\theta_0)-\exp(\alpha\zeta_2\sin\theta_0)]}{2},$$
$$T_2'(4,4)=\frac{\exp(-\alpha\zeta_2\sin\theta_0)+\exp(\alpha\zeta_2\sin\theta_0)}{2}. \tag{A.2}$$

Appendix B

The elements of the transfer matrices of two sub-cells in the ith unit cell of disordered periodic purely elastic structures are written as

$$T_1'(1,1)=\frac{\exp(-\mathrm{i}\alpha q_1\zeta_1)+\exp(\mathrm{i}\alpha q_1\zeta_1)}{2},\quad T_1'(1,2)=\frac{\exp(\mathrm{i}\alpha q_1\zeta_1)-\exp(-\mathrm{i}\alpha q_1\zeta_1)}{2\mathrm{i}\alpha q_1c_{44}^{(1)}},$$
$$T_1'(2,1)=\frac{\mathrm{i}\alpha q_1c_{44}^{(1)}[\exp(\mathrm{i}\alpha q_1\zeta_1)-\exp(-\mathrm{i}\alpha q_1\zeta_1)]}{2}, \tag{B.1}$$
$$T_1'(2,2)=\frac{\exp(-\mathrm{i}\alpha q_1\zeta_1)+\exp(\mathrm{i}\alpha q_1\zeta_1)}{2};$$

$$
\begin{aligned}
&T'_2(1,1) = \frac{\exp(-\mathrm{i}\alpha q_2\zeta_2) + \exp(\mathrm{i}\alpha q_2\zeta_2)}{2}, \quad T'_2(1,2) = \frac{\exp(\mathrm{i}\alpha q_2\zeta_2) - \exp(-\mathrm{i}\alpha q_2\zeta_2)}{2\mathrm{i}\alpha q_2 c_{44}^{(2)}}, \\
&T'_2(2,1) = \frac{\mathrm{i}\alpha q_2 c_{44}^{(2)}[\exp(\mathrm{i}\alpha q_2\zeta_2) - \exp(-\mathrm{i}\alpha q_2\zeta_2)]}{2}, \\
&T'_2(2,2) = \frac{\exp(-\mathrm{i}\alpha q_2\zeta_2) + \exp(\mathrm{i}\alpha q_2\zeta_2)}{2}.
\end{aligned} \tag{B.2}
$$

References

Baz, A., 2001. Active control of periodic structures. ASME, Journal of Vibration and Acoustics 123, 472–479.

Castanier, M.P., Pierre, C., 1995. Lyapunov exponents and localization phenomena in multi-coupled nearly periodic systems. Journal of Sound and Vibration 183, 493–515.

Castillero, J.B., Otero, J.A., Ramos, R.R., 1998. Asymptotic homogenization of laminated piezocomposite materials. International Journal of Solids and Structures 35, 527–541.

Hyland, D.C., Davis, L.D., 2002. Toward self-reliant control for adaptive structures. Acta Astronautica 51, 89–99.

Kissel, G.J., 1991. Localization factor for multichannel disordered systems. Physical Review A 44, 1008–1014.

Li, F.M., Hu, C., Huang, W.H., 2002. One-dimensional localization of elastic waves in rib-stiffened plates. Chinese Journal of Aeronautics 15, 208–212.

Li, F.M., Wang, Y.S., Hu, C., Huang, W.H., 2004. Localization of elastic waves in randomly disordered multi-coupled multi-span beams. Waves in Random Media 14, 217–227.

Otero, J.A., Calás, H., Rodríguez-Ramos, R., Maugin, G.A., Monsiváis, G., Pérez-Alvarez, R., 2004. Diffraction of transverse horizontal waves in Fibonacci piezoelectric superlattices. Zeitschrift für angewandte Mathematik und Physik ZAMP 55, 519–533.

Qian, Z.H., Jin, F., Wang, Z.K., Kishimoto, K., 2004. Dispersion relations for SH-wave propagation in periodic piezoelectric composite layered structures. International Journal of Engineering Science 42, 673–689.

Rodríguez-Ramos, R., Monsivais, G., Otero, J.A., Calás, H., Guerra, V., Stern, C., 2004. Presence of Stark ladders in scattering of shear horizontal piezoelectric waves. Journal of Applied Physics 96, 1178–1185.

Thorp, O., Ruzzene, M., Baz, A., 2001. Attenuation and localization of wave propagation in rods with periodic shunted piezoelectric patches. Smart Materials and Structures 10, 979–989.

Wolf, A., Swift, J.B., Swinney, H.L., Vastano, J.A., 1985. Determining Lyapunov exponents from a time series. Physica D 16, 285–317.

Xie, W.C., 1998. Buckling mode localization in rib-stiffened plates with randomly misplaced stiffeners. Computers and Structures 67, 175–189.

Xie, W.C., Ibrahim, A., 2000. Buckling mode localization in rib-stiffened plates with misplaced stiffeners—a finite strip approach. Chaos, Solitons and Fractals 11, 1543–1558.

Zinchuk, L.P., Podlipenets, A.N., 2001. Dispersion equations for Rayleigh waves in a piezoelectric periodically layered structure. Journal of Mathematical Sciences 103, 398–403.

Zingales, M., Elishakoff, I., 2000. Localization of the bending response in presence of axial load. International Journal of Solids and Structures 37, 6739–6753.